
Propagating Uncertainty through the tanh Function with Application to Reservoir Computing

Manan Gandhi

Georgia Institute of Technology
mgandhi@gatech.edu

Keuntaek Lee

Georgia Institute of Technology
keuntaek.lee@gatech.edu

Yunpeng Pan

JD.COM American Technologies Corporation
yunpeng.pan@jd.com

Evangelos A. Theodorou

Georgia Institute of Technology
evangelos.theodorou@gatech.edu

Abstract

Many neural networks use the tanh activation function, however when given a probability distribution as input, the problem of computing the output distribution in neural networks with tanh activation has not yet been addressed. One important example is the initialization of the echo state network in reservoir computing, where random initialization of the reservoir requires time to wash out the initial conditions, thereby wasting precious data and computational resources. Motivated by this problem, we propose a novel solution utilizing a moment based approach to propagate uncertainty through an Echo State Network to reduce the washout time. In this work, we contribute two new methods to propagate uncertainty through the tanh activation function and propose the Probabilistic Echo State Network (PESN), a method that is shown to have better average performance than deterministic Echo State Networks given the random initialization of reservoir states. Additionally we test single and multi-step uncertainty propagation of our method on two regression tasks and show that we are able to recover similar means and variances as computed by Monte-Carlo simulations.

1 Introduction

Neural networks can often have inputs that are uncertain. Input uncertainty can come from measurement error, adversarial noise [1], or even from output feedback. The majority of work on the subject of uncertainty in neural networks revolves around uncertainty in the model, not necessarily uncertainty in the input itself. Bayesian neural networks perform inference using a prior over the weights of the network, while dropout [2] samples iterations of the network with a probabilistic mask to build the posterior distribution of the model. In both cases the output uncertainty emerges as an explicit function of the model uncertainty, while the uncertainty of the input is classified as aleatoric and not explicitly propagated through the model. For non-parametric probabilistic methods, such as Gaussian process regression [3], special care must be taken for multi-step prediction with uncertain inputs [4]. In this paper, we focus on addressing the problem of uncertainty propagation through the tanh function, which is a popular choice for activation function in neural networks, in particular the Echo State Network.

In light of the challenges in input uncertainty propagation and their role in recurrent neural networks, we aim to contribute the following:

- A theoretical and numerical analysis for 3 methods of propagating input uncertainty through the tanh activation function, with an extension to other nonlinear activation functions.

Preprint. Work in progress.

- A new method, named the Probabilistic Echo State Network (PESN), which aims to reduce the time required to achieve the echo state property.

Related Works: There exists recent work on propagating input uncertainty through feed-forward bayesian neural networks [5]. Here, the authors perform approximate inference to propagate uncertain inputs through feedforward neural networks for classification tasks. We differentiate our work in three fundamental ways: 1) we consider the tanh function which is not addressed in [5], 2) a novel contribution utilizing splines to propagate gaussian input uncertainty through continuous activations and 3) a general focus on improving the reservoir computing framework. To the best of the authors' knowledge we are the first to utilize a spline approximation to the integrand of an expectation of a gaussian in order to perform approximate inference. Similar ideas include [6], where the authors utilize b-splines to approximate the density in order to perform approximate inference. Work in improving reservoir computing has traditionally focused on the structure of the reservoir, such as optimizing hyperparameters [7] or finding the minimum reservoir size [8]. This work is one of the first to attempt to reduce the time required to converge to the echo state property.

1.1 Reservoir Computing

Reservoir computing (RC) is a paradigm for training recurrent neural networks (RNNs) [9]. It was introduced in early 2000's by Jaeger under the name 'Echo State Networks' (ESN) for time-series predictions [10], and by Maass under the name 'Liquid State Machines' [11] for modeling computation in biological networks of neurons. Despite being developed from very different communities, these two approaches are largely mathematically identical. In this work we focus on ESN since we aim to improve the efficiency of RNN learning for engineering applications.

ESN differs from other RNNs in terms of its training scheme. Generally, RC consists of two steps: 1) drive a network with sparse and fixed connections with an input and output sequence. 2) Train the output (or readout) layer so that the network output is similar to the teacher output. The readout layer is usually trained using regression techniques such as linear regression [9] and Gaussian process regression [12]. One problem is determining the initial state of the hidden layer (reservoir). According to the echo state property [13], the effect of initial conditions can be 'washed out' therefore the state can be initialized randomly. However, there are three main drawbacks: first, a significant amount of training data is wasted because the initial period of training run needs to be discarded. Second, at test time, an initial input sequence needs to be fed into the network before using it for prediction tasks. Third, the state forgetting property is usually not guaranteed so the performance of the ESN may still depend on the initial state.

2 Propagating Uncertainty through the tanh

In our work we analyze three distinct methods to propagate a gaussian input through the tanh activation function. The simplest and most well known method is simply Monte-Carlo (MC) sampling where we sample the input distribution then pass each sample through the activation to compute an estimate of the moments. While easy to implement and understand, Monte Carlo has an obvious drawback in terms of computational time. The second method utilizes a well known approximation to the tanh activation function in the form of the logistic cumulative distribution function. The connection between the logistic and gaussian distributions are utilized to approximate the mean of the activation output. The variance approximation fits the moments of the Gaussian pdf to the function $(1 - \tanh(x)^2)$ in order to make the expectation tractable. The cross covariance terms are ignored in our derivation. While this method is certainly faster, the accuracy is limited by our approximations. The final method leverages spline approximations and analytical expressions for the expectation of polynomial functions. This method strikes a balance between computational complexity and accuracy by adjusting the width of the spline mesh. We compare absolute error of the moment approximations, computational complexity of the two analytical and spline methods, and provide error bounds for the spline approximation.

2.1 Analytical Approximation to Mean and Variance

First we relate the tanh function with the logistic cumulative distribution function CDF, and approximate the logistic distribution with an appropriate gaussian distribution. We assume that the

dimensions of the logistically distributed random vector x are independent given the location parameter z . The expectation and variance of x given z are $\mathbf{E}(x|z) = z$, $\mathbf{Var}(z|z) = \frac{\pi^2}{12}\mathbf{I}$ respectively. We can use moment matching to approximate x with a gaussian

$$p(x \geq 0|\lambda, \xi) = \frac{1}{1 + \exp(-\frac{\lambda}{\xi})} \quad (1)$$

$$\implies \tanh(z) = 2\left(\frac{1}{1 + \exp(-2z)}\right) - 1 \quad (2)$$

$$= 2p(x \geq 0|z, 0.5) - 1 \quad (3)$$

Here the logistic distribution is parameterized by the location λ and the scale ξ . The tanh function is a function of a logistic CDF with location $\lambda = z$ and scale $\xi = 0.5$. Additionally let us assume that $z \sim \mathcal{N}(\boldsymbol{\mu}, \boldsymbol{\sigma})$. The mean of the distribution, $p(\tanh(z))$, is given by:

$$\mathbf{E}(\tanh(z)) \approx \frac{2}{1 + \exp(-\frac{\boldsymbol{\mu}_i}{\sqrt{\frac{3}{\pi^2}\boldsymbol{\sigma}_i + \frac{1}{4}}})} - 1 = \mu_{\tanh(z_i)} \quad , \quad \text{for the } i^{\text{th}} \text{ element of } z \quad (4)$$

Next, we ignore the cross covariance terms between the elementwise tanh, and directly compute the diagonals of the output covariance matrix. The authors in [14] investigated different approximations to the error function. One preliminary solution was the use of the tanh function to approximate the error function. We can take advantage of this approximation and the appropriate scaling factors to approximate the function $(1 - \tanh(x))^2$. We use a Gaussian pdf where $\sigma^2 = \frac{2}{\pi}$ and $y = \frac{2}{\sqrt{\pi}}x$. Then we can again apply similar algebraic manipulations to compute the variance terms. The full derivation for the mean and variance expressions can be found in the supplementary material.

$$\frac{2}{\sqrt{2\pi\sigma^2}} \exp(-\frac{y^2}{2\sigma^2}) \approx (1 - \tanh(y^2)) \quad (5)$$

$$\mathbf{Var}(\tanh z_i) \approx 1 - \frac{2}{\sqrt{2\pi(\frac{2}{\pi} + \boldsymbol{\sigma}_{ii})}} \exp(-\frac{\boldsymbol{\mu}_i^2}{2(\frac{2}{\pi} + \boldsymbol{\sigma}_{ii})}) - \mu_{\tanh(z_i)}^2 \quad (6)$$

2.2 Spline Approximation to Mean and Variance

In this section, we present a formulation for computing the moments of the tanh transformation utilizing a spline approximation of the argument of the expectation. Again let us assume that $z \sim \mathcal{N}(\boldsymbol{\mu}, \boldsymbol{\sigma})$, the expectation and variance of the elementwise tanh are given by the following equations:

$$\mathbf{E}(\tanh(z_i)) = \int_{-\infty}^{\infty} \tanh(z_i) \frac{1}{\sqrt{2\pi\sigma_i}} \exp\left(-\frac{1}{2\sigma}(z_i - \mu_i)^2\right) dz_i \quad (7)$$

$$\begin{aligned} \mathbf{E}(\tanh(z_i) - \mathbf{E}(\tanh(z_i)))^2 &= 1 - \int_{-\infty}^{\infty} (1 - \tanh(z_i))^2 \frac{1}{\sqrt{2\pi\sigma_i}} \exp\left(-\frac{1}{2\sigma}(z_i - \mu_i)^2\right) dz_i - \\ &\quad - \mathbf{E}(\tanh(z_i))^2 \end{aligned} \quad (8)$$

Let us assume that we are dealing with scalar inputs to the activation function, since the vector case is handled elementwise and we are ignoring the off-diagonal elements of the input variance. Instead of direct numeric integration, we propose taking advantage of three facts.

- The tails of the Gaussian pdf approach zero, thus when multiplied against a function with constant tails, such as the tanh, the integrand also goes to zero. Thus we can approximate the integral over the real line using an integral over some compact subset centered around the mean of the input.
- The tanh function is continuous so we can uniformly approximate it with polynomials on the compact subset of integration.
- We can derive analytic forms for the definite integral of a product of polynomials and exponentials.

As a result, we can derive expressions for the mean and variance in terms of these analytic integrals. Let $f(z)$ be a scalar valued function that is continuous on the real interval $[a, b]$. Additionally, let $P(z)$ be a piecewise continuous cubic polynomial that interpolates f with N nodes, where each node is the beginning of intervals $[z_j, z_{j+1}]$, where $z_0 = a$ and $z_N = b$.

$$\mathbf{E}(f(z)) \approx \frac{1}{\sqrt{2\pi\sigma}} \int_a^b P(z) \exp\left(\frac{-1}{2\sigma}(z - \mu)^2\right) dz \quad (9)$$

$$= \frac{1}{\sqrt{2\pi\sigma}} \sum_{j=0}^{N-1} \int_{z_j}^{z_{j+1}} P(z) \exp\left(\frac{-1}{2\sigma}(z - \mu)^2\right) dz \quad (10)$$

$$= \frac{1}{\sqrt{2\pi\sigma}} \sum_{j=0}^{N-1} \int_{z_j}^{z_{j+1}} \sum_{k=0}^3 c_{jk} z^k \exp\left(\frac{-1}{2\sigma}(z - \mu)^2\right) dz \quad (11)$$

$$= \frac{1}{\sqrt{2\pi\sigma}} \sum_{j=0}^{N-1} \sum_{k=0}^3 c_{jk} \int_{z_j}^{z_{j+1}} z^k \exp\left(\frac{-1}{2\sigma}(z - \mu)^2\right) dz \quad (12)$$

Within the inner sum, the four terms can be computed analytically utilizing expressions for the integral of the product between polynomials and exponentials. We provide the full expressions for polynomials up to 3rd order in the supplementary material. The nodes and coefficients can be computed prior to evaluation of the network, and the integrals are computed once at every layer. This method is in fact general for any continuous function $f(z)$ whose tails are bounded, or polynomial outside of a compact set. Additionally, we can move forward to approximate higher moments of the output distribution and get expressions for the skew and kurtosis, at the cost of having spline approximations for $f(z)^3$ and $f(z)^4$. We provide expressions for higher moments and for alternative activation functions in the supplement. The mean and variance are given below, and Algorithm 1 describes how to use this technique to compute the moments of the activation.

$$\mu_{\tanh(\mu_i)} = A_1 \quad (13)$$

$$\sigma_{\tanh(\mu_i)} = A_2 - A_1^2 \quad (14)$$

$$A_1 = \int_{-\infty}^{\infty} f(z_i) \frac{1}{\sqrt{2\pi\sigma_i}} \exp\left(\frac{-1}{2\sigma_i}(z_i - \mu_i)^2\right) dz_i \quad (15)$$

$$A_2 = \int_{-\infty}^{\infty} f(z_i)^2 \frac{1}{\sqrt{2\pi\sigma_i}} \exp\left(\frac{-1}{2\sigma_i}(z_i - \mu_i)^2\right) dz_i \quad (16)$$

2.3 Computational Complexity Analysis

Next we look at the computational complexity of both the analytical and spline method in terms of the number of hidden states in the network. Let D be the number of hidden states in the network and let N be the number of mesh points for the spline approximation. Since the spline method makes frequent use of the error function, to approximate the operation count, we use the error function approximation introduced in [15]. We can see from Table 1 that if we use the spline approximation of \tanh , the time complexity is $\mathcal{O}(ND)$, while the analytical approximation of \tanh has the complexity of $\mathcal{O}(D)$. If we choose a fixed number of Monte Carlo samples M , then the Monte Carlo method is also linear with respect to reservoir D since the \tanh activation is element-wise and cross correlations are ignored. All 3 are linear in reservoir size and in practice we can see the this behavior of all 3 methods in Figure 2.

2.4 Error Bounds for Mean and Variance Estimation

In this section we provide an upper bound on the mean and variance estimates as a function of the input mean, input variance, the number of nodes in the mesh, and the location of the mesh in space. Let $g(z) \in \mathcal{C}^4$, and define τ as the maximum interval length in the mesh spanning some compact set $z \in [a, b]$. Then for a cubic spline approximation $P(z)$, we can place an upper bound on the maximum error over the interval $[a, b]$ [17].

$$\|g(z) - P(z)\|_{\infty} \leq \frac{1}{16} \tau^4 \|g^{(4)}(z)\|_{\infty}, \quad z \in [a, b], \quad \tilde{g}(z) = \begin{cases} -1 & , z \in (-\infty, a) \\ P(z) & , z \in [a, b] \\ 1 & , z \in (b, -\infty) \end{cases} \quad (17)$$

Algorithm 1 (μ, σ) approximation of $\tanh(z)$ with spline method

Input: a, b, n_{points}
1: $z \leftarrow$ evenly spaced n_{points} numbers over the interval $[a, b]$
2: $c_1, c_2 \leftarrow$ cubic spline coefficients of $\tanh(z), \tanh(z)^2$, where $P_i(z) = -c_{i,0}z^3 + c_{i,1}z^2 - c_{i,2}z + c_{i,3}$ ($i = 1, 2$)
3: **for** $j = 0$ to $n_{\text{points}} - 1$ **do**
4: $\alpha_j, \beta_j \leftarrow \frac{(z_j - \mu)}{\sqrt{2\sigma}}, \frac{(z_{j+1} - \mu)}{\sqrt{2\sigma}}$
5: $\mu_j \leftarrow$ Calculate Eq. (77) using Eq. (68)
6: $\sigma_j \leftarrow$ Calculate Eq. (78) using Eqs. (68), (77)
7: **end for**

Let us use $g(z) = \tanh(z)$. Given the fact that $z \sim \mathcal{N}(\mu, \sigma)$, we can compute an error bound over the mean of the output distribution by applying the triangle inequality.

$$\left| \int_{-\infty}^{\infty} (g(z) - \tilde{g}(z)) \frac{1}{\sqrt{2\pi\sigma}} \exp\left(\frac{-1}{2\sigma}(z - \mu)^2\right) dz \right| \leq c_1 \left(\operatorname{erf}\left(\frac{b - \mu}{\sqrt{2\sigma}}\right) - \operatorname{erf}\left(\frac{a - \mu}{\sqrt{2\sigma}}\right) \right) + c_2 \left(\operatorname{erf}\left(\frac{a - \mu}{\sqrt{2\sigma}}\right) + 1 \right) + c_3 \left(1 - \operatorname{erf}\left(\frac{b - \mu}{\sqrt{2\sigma}}\right) \right) = \epsilon_\mu \quad (18)$$

where $c_1 = \frac{1}{32}\tau^4 \|g^{(4)}(z)\|_\infty$, $c_2 = \frac{|1 + \tanh(a)|}{2}$, $c_3 = \frac{|\tanh(b) - 1|}{2}$. Let us additionally compute a bound for the variance. Let μ_{true} denote the true value of the mean, μ_{spline} be the approximated value of the mean. Additionally, let $\tilde{g}(z)$ be our polynomial approximation of $\tanh(z)^2$. Then we go to the expression for variance Equation (78):

$$\begin{aligned} \left| (\mathbf{E}((\tanh z)^2) - \mu_{\text{true}}^2) - (\mathbf{E}(\tilde{g}(z)) - \mu_{\text{spline}}^2) \right| &\leq \left| \mathbf{E}((\tanh z)^2 - \tilde{g}(z)) \right| + \left| \mu_{\text{spline}}^2 - \mu_{\text{true}}^2 \right| \\ &\leq \epsilon_1 + \left| (\mu_{\text{spline}} - \mu_{\text{true}})(\mu_{\text{spline}} + \mu_{\text{true}}) \right| \\ &\leq \epsilon_1 + 2\epsilon_\mu = \epsilon_\sigma \end{aligned} \quad (19)$$

ϵ_1 is the spline error bound where the unknown function is $\tanh(z)^2$. Additionally, we know that $|\mu_{\text{spline}} - \mu_{\text{true}}| < \epsilon_\mu(a, b, \mu, \sigma, \tau)$ and that since we are dealing with the tanh activation function, the activation mean is upper bounded by 1. Utilizing this method allows us to design the number of uniformly spaced mesh points and the size of the interval according to a desired accuracy. For reference, we utilize the interval $[-10, 10]$ for the mean of the tanh activation, and use 101 mesh points, resulting in an error bound of $4.21321e-5$ for the mean of an input distribution with mean 3 and variance 0.2. Again, the full derivation for both error bounds can be found in the supplement.

3 Probabilistic Echo State Networks

The proposed algorithm, Probabilistic Echo State Networks (PESN) derives its internal equations from the deterministic echo state network [13]. Let $z_k \in \mathbb{R}^{N_x + N_u}$ be input to the network, $y_k \in \mathbb{R}^{N_x}$ be the output of the network, $h_k \in \mathbb{R}^{N_h}$ is the hidden state at time k . The deterministic echo state network is characterized by 5 hyperparameters: reservoir size N_h , leak rate L , noise magnitude M_e , sparsity fraction s , and spectral radius r .

$$h_k = (1 - L)h_{k-1} + L \tanh(W_{\text{in}}z_k + W_{\text{fb}}y_{k-1} + Wh_{k-1}) + M_e dw \quad (20)$$

$$y_k = W_{\text{out}} [1 \quad z_k^T \quad h_k^T]^T \quad (21)$$

Here dw is Gaussian noise with variance 1. The sparsity fraction refers to the fraction on nonzero elements in the matrix W , while the spectral radius parameter is the spectral radius of W . For the

Table 1: Typical operation counts for the $\tanh(z)$ approximation

(a) Spline approximation				
Line	Algorithm 1			
	*/ \div	+/ $-$	<i>exp</i>	<i>sqrt</i>
1	2N	3N		
2[16]	28N	20N		
4	4ND	2ND		2ND
5	112ND	60ND	18ND	6ND
6	112ND+2	60ND+1	18ND	6ND
	228ND+30N+2	122ND+23N+1	36ND	14ND

(b) Analytical approximation				
Eq.	Eqs. (53), (62)			
	*/ \div	+/ $-$	<i>exp</i>	<i>sqrt</i>
Eq. (53)	6D	3D	1D	1D
Eq. (62)	17D	7D	2D	2D
	23D	10D	3D	3D

echo state network, we randomly generate the internal weight matrices W_{in} , W_{fb} , and W , and we only train the readout weight matrix W_{out} . In our case, training is accomplished using batch least squares. At test time, we recursively update the readout matrix using recursive least squares regression. [18]

For probabilistic echo state networks, assume that the input to the networks are Gaussian. We use moment matching to propagate the Gaussian uncertainty through the nonlinearity in the network, thus we retrieve a Gaussian output. Our notation is as follows: a Gaussian random vector z has a mean μ_z and covariance matrix Σ_z . We assume that all Gaussian vectors in our echo state network are additionally jointly Gaussian, so that linear combinations of these Gaussian vectors produce another Gaussian vector with appropriate mean vector and covariance matrix. Define the input as $z(k)$, the previous target as $y(k-1)$ and the hidden state as $h(k-1)$.

$$\mu_{\mathbf{a}} = W_{\text{in}}\mu_{z(k)} + W_{\text{fb}}\mu_{y(k-1)} + W\mu_{h(k-1)} \quad (22)$$

$$\begin{aligned} \Sigma_{\mathbf{a}} = & W_{\text{in}}\Sigma_{z(k)}W_{\text{in}}^T + W_{\text{fb}}\Sigma_{y(k-1)}W_{\text{fb}}^T + W\Sigma_{h(k-1)}W^T \\ & + 2W_{\text{in}}\Sigma_{z(k)y(k-1)}W_{\text{fb}}^T + 2W_{\text{fb}}\Sigma_{y(k-1)h(k-1)}W^T + 2W\Sigma_{h(k-1)z(k)}W_{\text{in}}^T \end{aligned} \quad (23)$$

Using our element-wise approximation, we drop the off-diagonal terms in \mathbf{a} and compute the approximate mean $\mu_{\text{tanh}(\mathbf{a})}$ and variance $\Sigma_{\text{tanh}(\mathbf{a})}$ using Equations (77) and (78). We also ignore the cross correlation terms, which will cause underestimation of uncertainty.

$$\mu_{h(k)} = (1-L)\mu_{h(k-1)} + L\mu_{\text{tanh}(\mathbf{a})} \quad (24)$$

$$\Sigma_{h(k)} = (1-L)^2\Sigma_{h(k-1)} + L^2\Sigma_{\text{tanh}(\mathbf{a})} + 2(1-L)L\Sigma_{\text{tanh}(\mathbf{a})h(k-1)} + M_e\mathbf{I} \quad (25)$$

$$\mathbf{b} = [1, z^T, h^T]^T \quad (26)$$

$$\mu_{y(k)} = W_{\text{out}}\mu_{\mathbf{b}} \quad (27)$$

$$\Sigma_{y(k)} = W_{\text{out}}\Sigma_{\mathbf{b}}W_{\text{out}}^T \quad (28)$$

Here (N_h, L, M_e, s, r) are the five hyperparameters for the echo state network, z and y are input and output data, generated or collected from experiments, n_{train} and n_{test} are the lengths of the train and test data, λ is a forgetting factor, P is $\delta\mathbf{I}$ where \mathbf{I} is the identity matrix. Algorithm 2 is used for training. Algorithm 3 is used for single and multi-step prediction for the probabilistic echo state network.

Algorithm 2 Training the PESN

Input: $N_h, L, M_e, s, r, z_{\text{train}}, y_{\text{train}}, N_{\text{washout}}$
1: Randomly initialize W, W_{in} and W_{fb}
2: Make some elements of W zero to have sparsity fraction of s
3: $W \leftarrow W * r / \max(\text{eigenvalue}(W))$
4: Initialize hidden state with Gaussian distribution
5: **for** $k = 1$ to n_{washout} **do**
6: Calculate $\mu_{h(k)}$ using Eq. (105)
7: **end for**
8: **for** $k = 1$ to n_{train} **do**
9: Calculate $\mu_{h(k)}$ using Eq. (105)
10: **end for**
11: $Z_{\text{train}} \leftarrow [1, z_{\text{train}}^T, \mu_{h(k)}^T]^T$
12: $W_{\text{out}} \leftarrow y_{\text{train}} Z_{\text{train}}^T (Z_{\text{train}} Z_{\text{train}}^T)^{-1}$

Algorithm 3 PESN single/multi step prediction

Input: $W_{\text{out}}, W_{\text{in}}, N_h, L, M_e, z_{\text{test}}, y_{\text{test}}, \lambda, P$
1: **for** $k = 1$ to n_{washout} **do**
2: Calculate $\mu_{h(k)}$ using Eq. (105)
3: **end for**
4: **for** $k = 1$ to n_{test} **do**
5: Calculate $\mu_{h(k)}$ and $\sigma_{h(k)}$ using Eqs. (102) - (106)
6: $B \leftarrow [1, z_{\text{test}}^T(k), \mu_{h(k)}^T]^T$
7: Calculate $\mu_{y(k)}$ and $\sigma_{y(k)}$ using Eqs. (108) and (109)
8: Incrementally update W_{out} and P
9: **if** single step prediction **then**
10: $y(k) \leftarrow y_{\text{test}}(k)$
11: **else**
12: $y(k) \leftarrow \mu_{y(k)}$
13: **end if**
14: **end for**

4 Experimental Evaluation

4.1 Numerical Analysis of Moment Approximation

First we compare the absolute error between the mean and variance estimated from Monte Carlo against the mean and variance from spline method and analytic method. We evaluate our moment propagation on a range input means and select variance values to assess accuracy. At each point, we have an input Gaussian distribution determined by a mean and variance. We sample this input distribution and compute an estimated mean and variance through Monte Carlo, then compare our two methods. Figure 4 shows that the spline method results in a more accurate approximation, and as the input saturates (mean approaches 5 and -5), the error quickly drops. In general we see the analytic approximation over estimates the variance of the tanh output. Full contour plots of the spline

and analytical comparison for a grid of both means and variance are available in the supplementary materials. We see in Figure 3 how computational time effects absolute error of moments. The analytic method is constant, but has comparatively high error compared to the others. The spline method has higher initial computational cost, but converges in error quickly.

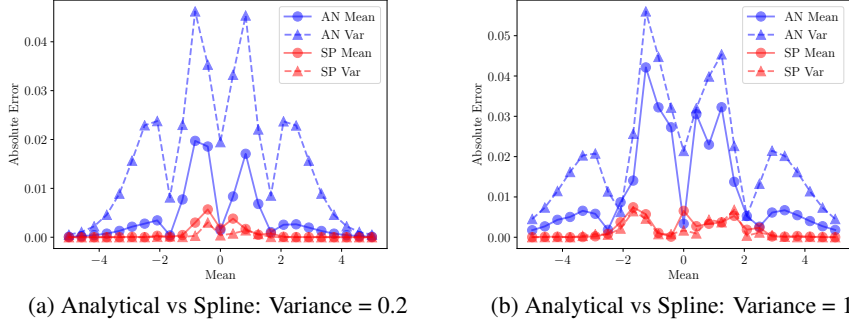


Figure 1: Comparison between the analytic (blue) and spline (red) for small and large variance for mean = -5 to 5.

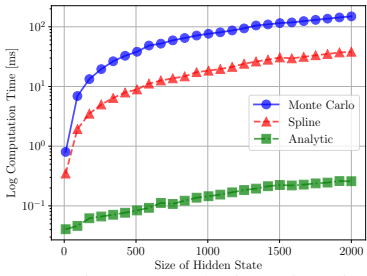


Figure 2: Time Complexity Visualization for Monte Carlo (1e4 Samples), Spline and Analytical Moments

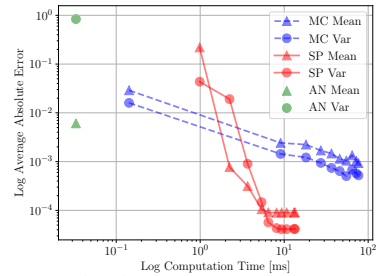


Figure 3: Absolute Error versus Computational Time for Monte Carlo and Spline and Analytical Moments

4.2 Effect of Probabilistic Hidden State on Washout Period

In Table 2 we numerically analyze the difference in multistep prediction error between the probabilistic echo state and the deterministic echo state algorithms as a function of the number of washout points. Each of the 50 trials were run with varying washout lengths (in timesteps), where we ran 50 samples of the deterministic echo state algorithm and compared the average absolute error between the ground truth and predicted state. The table shows the the probabilistic echo state network outperforms the monte-carlo deterministic echo state in absolute error for the majority of washout lengths. When the Monte Carlo deterministic ESN outperforms the PESN, it does so by a fairly small margin. This implies that the PESN reduces the time required to attain the “echo state property” that is characteristic for echo state networks.

Table 3: Absolute Error Statistics averaged over 50 trials of a 10 timestep trajectory of the Cart Pole. Lower entropy is bolded

Washout Length (timesteps)	Shannon Entropy Statistics					
	mean		min		max	
	P	MC	P	MC	P	MC
1	5.42	5.54	5.42	5.54	5.42	5.551
10	5.62	5.69	5.61	5.69	5.62	5.70
20	5.83	5.86	5.82	5.86	5.84	5.87
30	5.89	5.94	5.88	5.93	5.89	5.94
40	5.78	5.93	5.77	5.92	5.78	5.93
50	5.62	5.87	5.62	5.86	5.62	5.88
100	5.35	5.71	5.35	5.70	5.35	5.72
200	4.94	5.42	4.94	5.41	4.95	5.45

Table 2: Absolute Error Statistics averaged over 50 trials of a 10 timestep trajectory of the Cart Pole. In the “mean” column, the minimum value between probabilistic and monte-carlo is bolded. In the “Washout Length” column, the minimum error length is bolded.

(a) Position							(b) Velocity						
Washout Length (timesteps)	Error Statistics						Washout Length (timesteps)	Error Statistics					
	mean		min		max			mean		min		max	
	P	MC	P	MC	P	MC		P	MC	P	MC	P	MC
1	0.0093	0.0128	0.0088	0.0062	0.0134	0.0212	1	0.0369	0.0401	0.0249	0.0210	0.0381	0.0650
10	0.0135	0.0167	0.0134	0.0057	0.0135	0.0377	10	0.0203	0.0222	0.0201	0.0061	0.0203	0.0462
20	0.0428	0.0428	0.0428	0.0166	0.0429	0.0619	20	0.0159	0.0191	0.0159	0.0121	0.0159	0.0305
30	0.0836	0.0842	0.0836	0.0651	0.0836	0.1007	30	0.0573	0.0585	0.0573	0.0405	0.0573	0.0793
40	0.1379	0.1359	0.1379	0.1139	0.1379	0.1562	40	0.1247	0.1240	0.1247	0.0994	0.1247	0.1402
50	0.2084	0.2091	0.2083	0.1951	0.2084	0.2279	50	0.2206	0.2223	0.2206	0.2078	0.2206	0.2407
100	0.7138	0.7126	0.7138	0.6945	0.7138	0.7375	100	1.3919	1.3936	1.3919	1.3775	1.3919	1.4133
200	0.1525	0.1495	0.1525	0.1268	0.1525	0.1697	200	4.4890	4.4887	4.4890	4.4707	4.4890	4.5095

(c) Angle							(d) Angular Velocity						
Washout Length (timesteps)	Error Statistics						Washout Length (timesteps)	Error Statistics					
	mean		min		max			mean		min		max	
	P	MC	P	MC	P	MC		P	MC	P	MC	P	MC
1	0.3206	0.3578	0.0653	0.3401	0.3473	0.3808	1	0.7104	0.7633	0.3200	0.7406	0.7496	0.8063
10	0.4380	0.4464	0.4352	0.4230	0.4397	0.4657	10	0.6576	0.6652	0.6536	0.6430	0.6601	0.6931
20	0.5478	0.5496	0.5470	0.5283	0.5485	0.5685	20	0.5273	0.5298	0.5260	0.5058	0.5282	0.5597
30	0.6739	0.6756	0.6734	0.6511	0.6742	0.6955	30	0.3817	0.3834	0.3811	0.3599	0.3821	0.4063
40	0.8240	0.8240	0.8238	0.8045	0.8243	0.8416	40	0.2550	0.2558	0.2548	0.2361	0.2552	0.2769
50	1.0001	0.9997	0.9999	0.9803	1.0002	1.0169	50	0.2761	0.2759	0.2760	0.2687	0.2761	0.2871
100	0.7372	0.7356	0.7371	0.7130	0.7373	0.7562	100	2.8593	2.8619	2.8592	2.8388	2.8595	2.8920
200	0.7244	0.7245	0.7243	0.7053	0.7245	0.7531	200	2.6587	2.6594	2.6586	2.6350	2.6588	2.6916

In an attempt to quantify the level of synchronization in the hidden states of both the ESN and the PESN, we can create a probability distribution of the values of the reservoir values during washout. Synchronization would imply that there is less uncertainty in the values of the hidden state, thus we can quantify this via the Shannon Entropy of this probability distribution. Table 3 lists the Shannon entropy values for hidden state trajectories. Intuitively, the entropy is small for every washout length, which implies there is less randomness to “wash out”.

4.3 Model Learning

We test the PESN on the task of learning dynamics of cart pole and Gazebo ARDrone. We compare the PESN against Monte Carlo estimates obtained with the deterministic ESN. The PESN successfully propagates uncertainty for single step predictions and for up to 20 timesteps for multi step prediction. The results, found in the supplementary material Section 3.3, demonstrate the ability of our method to capture input uncertainty as it passes through the recurrent network.

5 Conclusions

In this work, we investigate two different methods of propagating uncertainty through the tanh function. We demonstrate that the analytical method is the fastest way to propagate uncertainty through the tanh function, however it tends to over estimate uncertainty. The spline method is more general and has tuneable accuracy, however the computational cost is higher. Utilizing these new developments, we propose the probabilistic echo state network (PESN), which attempts to solve a fundamental problem of reservoir computing, which is the time required to fulfill the asymptotic behavior of the echo state property. We are able demonstrate, for multi step regression tasks, the PESN has better performance than a deterministic ESN (as measured by absolute error). The better performance is accompanied by a lower shannon entropy in the distribution of hidden state value distribution, which we believe indicates faster convergence to the echo state property. We additionally test the PESN method on ARDrone data collected from the Gazebo simulator, to demonstrate that the method can scale to higher dimensional systems and still propagate uncertainty effectively. However, these methods are not without their drawbacks. For the spline method, input, output scaling and spectral radius of the PESN must be tuned fit inside interval $[a, b]$ so that we satisfy our moment error bounds. The multi-step regression is heavily dependent on incremental updating of the output weights in order to maintain low absolute error. Both the spline and analytic methods are tractable techniques to propagate uncertainty through the tanh function, and the resulting Probabilistic Echo State network is able to improve the convergence to the echo state property.

References

- [1] Christian Szegedy, Wojciech Zaremba, Ilya Sutskever, Joan Bruna, Dumitru Erhan, Ian Goodfellow, and Rob Fergus. Intriguing properties of neural networks. *arXiv preprint arXiv:1312.6199*, 2013.
- [2] Yarin Gal and Zoubin Ghahramani. A theoretically grounded application of dropout in recurrent neural networks. In *Advances in neural information processing systems*, pages 1019–1027, 2016.
- [3] Carl Edward Rasmussen. Gaussian processes in machine learning. In *Advanced lectures on machine learning*, pages 63–71. Springer, 2004.
- [4] Agathe Girard, Carl Edward Rasmussen, Joaquin Quinonero Candela, and Roderick Murray-Smith. Gaussian process priors with uncertain inputs application to multiple-step ahead time series forecasting. In *Advances in neural information processing systems*, pages 545–552, 2003.
- [5] Alexander Shekhovtsov, Boris Flach, and Michal Busta. Feed-forward uncertainty propagation in belief and neural networks. *arXiv preprint arXiv:1803.10590*, 2018.
- [6] Roland Langrock, Thomas Kneib, Alexander Sohn, and Stacy L DeRuiter. Nonparametric inference in hidden markov models using p-splines. *Biometrics*, 71(2):520–528, 2015.
- [7] Herbert Jaeger, Mantas Lukoševičius, Dan Popovici, and Udo Siewert. Optimization and applications of echo state networks with leaky-integrator neurons. *Neural networks*, 20(3):335–352, 2007.
- [8] Ali Rodan and Peter Tino. Minimum complexity echo state network. *IEEE transactions on neural networks*, 22(1):131–144, 2011.
- [9] Mantas Lukoševičius and Herbert Jaeger. Reservoir computing approaches to recurrent neural network training. *Computer Science Review*, 3(3):127–149, 2009.
- [10] Herbert Jaeger and Harald Haas. Harnessing nonlinearity: Predicting chaotic systems and saving energy in wireless communication. *Science*, 304(5667):78–80, 2004.
- [11] Wolfgang Maass, Thomas Natschläger, and Henry Markram. Computational models for generic cortical microcircuits. *Computational Neuroscience: A Comprehensive Approach*, pages 575–605, 2004.
- [12] Sotirios P Chatzis and Yiannis Demiris. Echo state gaussian process. *IEEE Transactions on Neural Networks*, 22(9):1435–1445, 2011.
- [13] Herbert Jaeger. The echo state approach to analysing and training recurrent neural networks—with an erratum note. *Bonn, Germany: German National Research Center for Information Technology GMD Technical Report*, 148(34):13, 2001.
- [14] Bruce Bassett. $e^{-x^2} dx$ and the kink soliton. *Computers & Mathematics with applications*, 36(4):37–45, 1998.
- [15] Milton Abramowitz and Irene A. Stegun. *Handbook of Mathematical Functions: With Formulas, Graphs, and Mathematical Tables*. Courier Corporation, 1964.
- [16] William H. Press, Saul A. Teukolsky, William T. Vetterling, and Brian P. Flannery. *Numerical recipes 3rd edition: the art of scientific computing*. Cambridge University Press, 2007.
- [17] Carl De Boor. *A practical guide to splines*. Springer-Verlag New York, 1978.
- [18] Dan Simon. *Optimal state estimation: Kalman, H infinity, and nonlinear approaches*. John Wiley & Sons, 2006.
- [19] Kaare Brandt Petersen, Michael Syskind Pedersen, et al. The matrix cookbook. *Technical University of Denmark*, 7(15):510, 2008.
- [20] J. Engel, J. Sturm, and D. Cremers. Camera-based navigation of a low-cost quadcopter. In *Proc. of the International Conference on Intelligent Robot Systems (IROS)*, 2012.

6 Supplementary Material

This is the supplementary material for the paper on Propagating Uncertainty through the Tanh function for Reservoir Computing. The supplement is organized as follows: Section 6.1 includes derivations for both the analytic and spline methods, derivations for the error bound for mean and variance of the spline tanh approximation. Section 6.2 repeats the equations for the Probabilistic Echo State Network (PESN). Section 6.3 contains additional numerical examples. These include propagation of uncertainty through a feedforward neural network for regression, dynamical systems regression, and activation function comparisons.

6.1 Propagating Uncertainty through Tanh

6.1.1 Analytical Approximation of Mean and Variance

First we present some useful identities and approximations: The cumulative distribution function (CDF) of a logistic distribution over a random variable x is:

$$F_x(\mathbf{a}) = \mathbb{p}(x \leq \mathbf{a}) = \frac{1}{1 + \exp(-\frac{\mathbf{a}-\lambda}{\sigma})} \implies \mathbb{p}(x \leq 0 | \lambda, \sigma) = \frac{1}{1 + \exp(\frac{\lambda}{\sigma})} \quad (29)$$

$$\implies \mathbb{p}(x \geq 0 | \lambda, \sigma) = \frac{1}{1 + \exp(-\frac{\lambda}{\sigma})} \quad (30)$$

Here the logistic distribution is parameterized by the location λ and the scale σ . The tanh function can be written as follows and relation can be derived:

$$\tanh(\mathbf{z}) = \frac{e^{\mathbf{z}} - e^{-\mathbf{z}}}{e^{\mathbf{z}} + e^{-\mathbf{z}}} \quad (31)$$

$$= \frac{1 - e^{-2\mathbf{z}}}{1 + e^{-2\mathbf{z}}} \quad (32)$$

$$= \frac{1 + 1 - (1 + e^{-2\mathbf{z}})}{1 + e^{-2\mathbf{z}}} \quad (33)$$

$$= \frac{2}{1 + e^{-2\mathbf{z}}} - \frac{1 + e^{-2\mathbf{z}}}{1 + e^{-2\mathbf{z}}} \quad (34)$$

$$= 2\left(\frac{1}{1 + \exp(-2\mathbf{z})}\right) - 1 \quad (35)$$

$$= 2\mathbb{p}(x \geq 0 | \mathbf{z}, 0.5) - 1 \quad (36)$$

Thus the tanh function is a function of a logistic CDF with location $\lambda = \mathbf{z}$ (the input to the tanh) and scale $\sigma = 0.5$. Let us assume that the dimensions of the logistically distributed random vector x are independent given the location parameter \mathbf{z} . From the definition of the logistic distribution, the mean and variance of the conditional distribution $\mathbb{p}(x | \mathbf{z}, 0.5)$ are:

$$\mathbf{E}(x | \mathbf{z}) = \mathbf{z}, \quad \mathbf{Var}(x | \mathbf{z}) = \frac{\pi^2}{12} \mathbf{I} \quad (37)$$

We also make use of the formula for the product of two Gaussian distributions ([19]).

$$\mathcal{N}_x(\mu_a, \Sigma_a) \times \mathcal{N}_x(\mu_b, \Sigma_b) = c \times \mathcal{N}_x(\mu_c, \Sigma_c) \quad (38)$$

where

$$c = \frac{1}{\sqrt{|2\pi(\Sigma_a + \Sigma_b)|}} \exp\left(-\frac{1}{2}(\mu_a - \mu_b)^T (\Sigma_a + \Sigma_b)^{-1} (\mu_a - \mu_b)\right) \quad (39)$$

$$\mu_c = (\Sigma_a^{-1} + \Sigma_b^{-1})^{-1} (\Sigma_a^{-1} \mu_a + \Sigma_b^{-1} \mu_b) \quad (40)$$

$$\Sigma_c = (\Sigma_a^{-1} + \Sigma_b^{-1})^{-1} \quad (41)$$

Let us assume that $\mathbf{z} \sim \mathcal{N}(\boldsymbol{\mu}, \boldsymbol{\sigma})$. We want to compute the moments of the distribution: $\mathbb{p}(\tanh(\mathbf{z}))$. We will make use of moment matching to approximate a logistic distribution with a Gaussian, and vice versa.

$$\mathbb{p}(x | \mathbf{z}, 0.5) \approx x | \mathbf{z}, 0.5 \sim \mathcal{N}\left(\mathbf{z}, \frac{\pi^2}{12} \mathbf{I}\right) \quad (42)$$

Mean: First we compute the mean of $p(\tanh(\mathbf{z}))$.

$$\mathbf{E}(\tanh(\mathbf{z})) = \int \tanh(\mathbf{z})p(\mathbf{z})d\mathbf{z} \quad (43)$$

$$\text{Eq (36)} \implies = \int (2p(x \geq 0|\mathbf{z}, 0.5) - 1)p(\mathbf{z})d\mathbf{z} \quad (44)$$

$$= 2 \int p(x \geq 0|\mathbf{z}, 0.5)p(\mathbf{z})d\mathbf{z} - 1 \quad (45)$$

$$\text{CDF Definition} \implies = 2 \int \left(\int_0^\infty p(x|\mathbf{z}, 0.5)dx \right) p(\mathbf{z})d\mathbf{z} - 1 \quad (46)$$

$$\text{Eq (42)} \implies \approx 2 \int \left(\int_0^\infty \mathcal{N}(z, \frac{\pi^2}{12}\mathbf{I})dx \right) p(\mathbf{z})d\mathbf{z} - 1 \quad (47)$$

$$\text{Distribution of } \mathbf{z} \implies = 2 \int \left(\int_0^\infty \mathcal{N}(z, \frac{\pi^2}{12}\mathbf{I})dx \right) \mathcal{N}(\boldsymbol{\mu}, \boldsymbol{\sigma})d\mathbf{z} - 1 \quad (48)$$

$$\text{Fubini's Theorem} \implies = 2 \int_0^\infty \left(\int \mathcal{N}(z, \frac{\pi^2}{12}\mathbf{I})\mathcal{N}(\boldsymbol{\mu}, \boldsymbol{\sigma})d\mathbf{z} \right) dx - 1 \quad (49)$$

$$\text{Eq (38)} \implies = 2 \int_0^\infty \left(\int (2\pi)^{\frac{n}{2}} |\boldsymbol{\sigma} + \frac{\pi^2}{12}\mathbf{I}|^{u\frac{1}{2}} p(\mathbf{z}) \times \right. \\ \left. \exp\left(-\frac{1}{2}(x - \boldsymbol{\mu})^T (\boldsymbol{\sigma} + \frac{\pi^2}{12}\mathbf{I})^{-1} (x - \boldsymbol{\mu})\right) d\mathbf{z} \right) dx - 1 \quad (50)$$

In Equation (50), we use the product rule of Gaussians, and specify: $\mu_a = x$, $\mu_b = \boldsymbol{\mu}$, $\Sigma_a = \mathbf{I}\frac{\pi^2}{12}$, and $\Sigma_b = \boldsymbol{\sigma}$. Then we are left with the constant coefficient in front of a Gaussian pdf of the input \mathbf{z} . As a result, the constant coefficient is not a function of the input, thus the integral over this Gaussian pdf integrates to 1.

$$\mathbf{E}(\tanh(\mathbf{z})) \approx 2 \int_0^\infty (2\pi)^{\frac{n}{2}} |\boldsymbol{\sigma} + \frac{\pi^2}{12}\mathbf{I}|^{\frac{1}{2}} \exp\left(-\frac{1}{2}(x - \boldsymbol{\mu})^T (\boldsymbol{\sigma} + \frac{\pi^2}{12}\mathbf{I})^{-1} (x - \boldsymbol{\mu})\right) dx - 1 \\ = 2 \int_0^\infty \mathcal{N}(\boldsymbol{\mu}, \boldsymbol{\sigma} + \frac{\pi^2}{12}\mathbf{I}) dz - 1 \quad (51)$$

$$\approx 2p(x \geq 0|\boldsymbol{\mu}, \sqrt{\frac{3}{\pi^2}}(\boldsymbol{\sigma} + \frac{\pi^2}{12}\mathbf{I})) - 1 \quad (52)$$

$$\text{Equation (30)} \implies = \frac{2}{1 + \exp\left(-\frac{\boldsymbol{\mu}_i}{\sqrt{\frac{3}{\pi^2}\boldsymbol{\sigma}_i + \frac{1}{4}}}\right)} - 1, \text{ for each element } i \text{ in } \mathbf{z} \quad (53)$$

Thus, given the input mean and diagonal covariance function, we can compute the posterior mean of an elementwise tanh operation.

Variance: The author in [14] investigated different approximations to the error function. One preliminary solution was the use of the tanh function to approximate the error function. Using this fact, we see that with the appropriate scaling factors, the Gaussian pdf can be an approximation to the function $(1 - \tanh(x))^2$. Again, we are ignoring cross correlation terms, thus the output variance will be diagonal and we can compute each term separately.

$$\text{erf}(x) \approx \tanh\left(\frac{2}{\sqrt{\pi}}x\right) \quad (54)$$

$$\implies \frac{d}{dx}\text{erf}(x) \approx \frac{d}{dx}\tanh\left(\frac{2}{\sqrt{\pi}}x\right) \quad (55)$$

$$\implies \frac{2}{\sqrt{2\pi\sigma^2}} \exp\left(-\frac{y^2}{2\sigma^2}\right) \approx (1 - \tanh(y^2)) \quad (56)$$

where $\sigma^2 = \frac{2}{\pi}$ and $y = \frac{2}{\sqrt{\pi}}x$.

$$\mathbf{Var}(\tanh \mathbf{z}_i) = \mathbf{E}(\tanh(\mathbf{z}_i)^2) - (\mathbf{E} \tanh(\mathbf{z}_i))^2 \quad (57)$$

$$= 1 - \mathbf{E}(1 - \tanh(\mathbf{z}_i)^2) - (\mathbf{E} \tanh(\mathbf{z}_i))^2 \quad (58)$$

$$\text{Eq (56)} \implies \approx 1 - \mathbf{E}\left(\frac{2}{\sqrt{2\pi\sigma^2}} \exp\left(-\frac{\mathbf{z}_i^2}{2\sigma^2}\right)\right) - (\mathbf{E} \tanh(\mathbf{z}_i))^2 \quad (59)$$

$$= 1 - 2 \int \mathcal{N}\left(0, \frac{2}{\pi}\right) \mathcal{N}(\boldsymbol{\mu}_i, \boldsymbol{\sigma}_{ii}) d\mathbf{z}_i - (\mathbf{E} \tanh(\mathbf{z}_i))^2 \quad (60)$$

$$\text{Eq (38)} \implies = 1 - 2 \int \frac{1}{\sqrt{2\pi\left(\frac{2}{\pi} + \boldsymbol{\sigma}_{ii}\right)}} \exp\left(-\frac{\boldsymbol{\mu}_i^2}{2\left(\frac{2}{\pi} + \boldsymbol{\sigma}_{ii}\right)}\right) p(\mathbf{z}_i) d\mathbf{z}_i - (\mathbf{E} \tanh(\mathbf{z}_i))^2 \quad (61)$$

$$= 1 - \frac{2}{\sqrt{2\pi\left(\frac{2}{\pi} + \boldsymbol{\sigma}_{ii}\right)}} \exp\left(-\frac{\boldsymbol{\mu}_i^2}{2\left(\frac{2}{\pi} + \boldsymbol{\sigma}_{ii}\right)}\right) - \left(\frac{2}{1 + \exp\left(-\frac{\boldsymbol{\mu}_i}{\sqrt{\frac{3}{\pi^2}\boldsymbol{\sigma}_i + \frac{1}{4}}}\right)} - 1\right)^2 \quad (62)$$

6.1.2 Spline Approximation of Mean and Variance

In this section, we present a formulation for computing the moments of the tanh transformation utilizing a spline approximation of the argument of the expectation. Again let us assume that $\mathbf{z} \sim \mathcal{N}(\boldsymbol{\mu}, \boldsymbol{\sigma})$, the expectation and variance of the elementwise tanh are given by the following equations:

$$\mathbf{E} \tanh(\mathbf{z}_i) = \int_{-\infty}^{\infty} \tanh(\mathbf{z}_i) \frac{1}{\sqrt{2\pi\sigma_i}} \exp\left(\frac{-1}{2\sigma} (\mathbf{z}_i - \mu_i)^2\right) d\mathbf{z}_i \quad (63)$$

$$\mathbf{E}(\tanh(\mathbf{z}_i) - \mathbf{E} \tanh(\mathbf{z}_i))^2 = 1 - \int_{-\infty}^{\infty} (1 - \tanh(\mathbf{z}_i)^2) \frac{1}{\sqrt{2\pi\sigma_i}} \exp\left(\frac{-1}{2\sigma} (\mathbf{z}_i - \mu_i)^2\right) d\mathbf{z}_i - \mathbf{E} \tanh(\mathbf{z}_i)^2 \quad (64)$$

In both cases the integrands are not easily integrable, and depend on the mean and variance of the input. Let us assume that we are dealing with scalar inputs to the activation function, since the vector case is handled elementwise and we are ignoring the off-diagonal elements of the input variance. Instead of direct numeric integration, we propose taking advantage of three facts. First, we know that the tails of the Gaussian pdf approach zero, thus when multiplied against a function with constant tails, the integrand also goes to zero. The tanh, *sigmoid* both have constant tails. For the *ReLU* and *swish* activation functions, the negative tail is 0, and the positive tail is x , which has an analytical form when integrated against a Gaussian. Thus we can approximate the integral over the real line using an integral over some compact subset centered around the mean of the input. Second, most activation functions are continuous, and on the compact subset of integration, we can uniformly approximate these functions with polynomials, in fact we will utilize piecewise cubic polynomials for this approximation. Finally, we can derive analytic forms to the integrals of polynomials multiplied against exponentials. The results are expressions for both the output mean and variance that are functions of the exponential function, error function, and input mean and variance. Let $f(z)$ be a scalar valued function that is continuous on the real interval $[a, b]$. Additionally, let $P(z)$ be a piecewise continuous cubic polynomial that interpolates f with N nodes, where each node is the

beginning of intervals $[z_j, z_{j+1}]$, where $z_0 = a$ and $z_N = b$.

$$\mathbf{E}f(z) \approx \frac{1}{\sqrt{2\pi\sigma}} \int_a^b P(z) \exp\left(\frac{-1}{2\sigma}(z - \mu)^2\right) dz \quad (65)$$

$$= \frac{1}{\sqrt{2\pi\sigma}} \sum_{j=0}^{N-1} \int_{z_j}^{z_{j+1}} P(z) \exp\left(\frac{-1}{2\sigma}(z - \mu)^2\right) dz \quad (66)$$

$$= \frac{1}{\sqrt{2\pi\sigma}} \sum_{j=0}^{N-1} \int_{z_j}^{z_{j+1}} \sum_{k=0}^3 c_{jk} z^k \exp\left(\frac{-1}{2\sigma}(z - \mu)^2\right) dz \quad (67)$$

$$= \frac{1}{\sqrt{2\pi\sigma}} \sum_{j=0}^{N-1} \sum_{k=0}^3 c_{jk} \int_{z_j}^{z_{j+1}} z^k \exp\left(\frac{-1}{2\sigma}(z - \mu)^2\right) dz \quad (68)$$

Within the inner sum, the four terms can be computed analytically, however let us first make a change of variables to simplify the expressions. Let $x = \frac{(z-\mu)}{\sqrt{2\sigma}}$, then $dz = \sqrt{2\sigma}dx$. Additionally we should transform our bounds: $\alpha = \frac{(z_j-\mu)}{\sqrt{2\sigma}}$ and $\beta = \frac{(z_{j+1}-\mu)}{\sqrt{2\sigma}}$. Next we can compute the integrals:

$$\frac{1}{\sqrt{2\pi\sigma}} \int_{z_j}^{z_{j+1}} \exp\left(\frac{-1}{2\sigma}(z - \mu)^2\right) dz = \frac{1}{\sqrt{\pi}} \int_{\alpha}^{\beta} \exp(-x^2) dx \quad (69)$$

$$= \frac{1}{2} (\operatorname{erf}(\beta) - \operatorname{erf}(\alpha)) \quad (70)$$

$$\frac{1}{\sqrt{2\pi\sigma}} \int_{z_j}^{z_{j+1}} z \exp\left(\frac{-1}{2\sigma}(z - \mu)^2\right) dz = \frac{1}{\sqrt{\pi}} \int_{\alpha}^{\beta} (x\sqrt{2\sigma} + \mu) \exp(-x^2) dx \quad (71)$$

$$= \sqrt{\frac{\sigma}{2\pi}} (\exp(-\alpha^2) - \exp(-\beta^2)) + \frac{\mu}{2} (\operatorname{erf}(\beta) - \operatorname{erf}(\alpha)) \quad (72)$$

$$\frac{1}{\sqrt{2\pi\sigma}} \int_{z_j}^{z_{j+1}} z^2 \exp\left(\frac{-1}{2\sigma}(z - \mu)^2\right) dz = \frac{1}{\sqrt{\pi}} \int_{\alpha}^{\beta} (x\sqrt{2\sigma} + \mu)^2 \exp(-x^2) dx \quad (73)$$

$$= \frac{\sigma}{2} (\operatorname{erf}(\beta) - \operatorname{erf}(\alpha)) + \frac{2}{\sqrt{\pi}} (\alpha \exp(-\alpha^2) - \beta \exp(-\beta^2)) + \sqrt{\frac{2\sigma}{\pi}} (\exp(-\alpha^2) - \exp(-\beta^2)) + \frac{\mu^2}{2} (\operatorname{erf}(\beta) - \operatorname{erf}(\alpha)) \quad (74)$$

$$\frac{1}{\sqrt{2\pi\sigma}} \int_{z_j}^{z_{j+1}} z^3 \exp\left(\frac{-1}{2\sigma}(z - \mu)^2\right) dz = \frac{1}{\sqrt{\pi}} \int_{\alpha}^{\beta} (x\sqrt{2\sigma} + \mu)^3 \exp(-x^2) dx \quad (75)$$

$$= \sqrt{\frac{2\sigma^3}{\pi}} ((1 + \alpha^2) \exp(-\alpha^2) - (1 + \beta^2) \exp(-\beta^2)) + \frac{3\sigma\mu}{\sqrt{\pi}} (\sqrt{\pi}(\operatorname{erf}(\beta) - \operatorname{erf}(\alpha)) + 2\alpha \exp(-\alpha^2) - 2\beta \exp(-\beta^2)) + 3\mu^2 \sqrt{\frac{\sigma}{2\pi}} (\exp(-\alpha^2) - \exp(-\beta^2)) + \frac{\mu^3}{2} (\operatorname{erf}(\beta) - \operatorname{erf}(\alpha)) \quad (76)$$

Thus using Equation (68), and Equations (70) - (76), we can analytically compute the expectation of any smooth function $f(z)$ whose tails are constant, or polynomial outside of a compact set. The

nodes and coefficients can be computed prior to evaluation of the network, and the integrals are computed once at every layer. The mean and variance the functions to approximate are $f(z)$ and $f(z)^2$ respectively. Both functions have a distinct set of coefficients, but we use the same set of equally spaced nodes for each of computation. Additionally, we can move forward to approximate higher moments of the output distribution and get expressions for the skew and kurtosis, at the cost of having spline approximations for $f(z)^3$ and $f(z)^4$. We can express the mean μ , variance σ , skewness γ and kurtosis κ .

$$\mu = A_1 \quad (77)$$

$$\sigma = A_2 - A_1^2 \quad (78)$$

$$\gamma = \frac{A_3 - 3A_1\sigma - A_1^3}{\sigma^{3/2}} \quad (79)$$

$$\kappa = \frac{A_4 - 4A_1A_3 + 6A_2^2A_1^2 - 3A_1^4}{\sigma^2} \quad (80)$$

where

$$A_1 = \int_{-\infty}^{\infty} f(z_i) \frac{1}{\sqrt{2\pi\sigma_i}} \exp\left(\frac{-1}{2\sigma}(z_i - \mu_i)^2\right) dz_i \quad (81)$$

$$A_2 = \int_{-\infty}^{\infty} f(z_i)^2 \frac{1}{\sqrt{2\pi\sigma_i}} \exp\left(\frac{-1}{2\sigma}(z_i - \mu_i)^2\right) dz_i \quad (82)$$

$$A_3 = \int_{-\infty}^{\infty} f(z_i)^3 \frac{1}{\sqrt{2\pi\sigma_i}} \exp\left(\frac{-1}{2\sigma}(z_i - \mu_i)^2\right) dz_i \quad (83)$$

$$A_4 = \int_{-\infty}^{\infty} f(z_i)^4 \frac{1}{\sqrt{2\pi\sigma_i}} \exp\left(\frac{-1}{2\sigma}(z_i - \mu_i)^2\right) dz_i \quad (84)$$

Error Bounds for Spline Mean and Variance Estimation: In this section we provide an upper bound on the mean and variance estimates as function of the input mean, input variance, the number of nodes in the mesh, and the location of the mesh in space. Let $g(z) \in C^4$ (some examples of common activation functions with fourth derivatives are tanh, linear, sigmoid, and swish), and define τ as the maximum interval length in the mesh spanning some compact set $z \in [a, b]$. Then for a cubic spline approximation $P(x)$, we can place an upper bound on the maximum error over the interval $[a, b]$ [17].

$$\|g(z) - P(z)\|_{\infty} \leq \frac{1}{16} \tau^4 \|g^{(4)}(z)\|_{\infty}, \quad z \in [a, b] \quad (85)$$

Let us use $g(z) = \tanh(z)$ as an example to compute an expression for the error for an approximation of $\mathbf{E} \tanh(z)$.

$$\tilde{g}(z) = \begin{cases} -1 & , z \in (-\infty, a) \\ P(z) & , z \in [a, b] \\ 1 & , z \in (b, -\infty) \end{cases} \quad (86)$$

Now we approximate expectation of the function $g(z)$, given the fact that $z \sim \mathcal{N}(\mu, \sigma)$, by splitting the integral into pieces where the function is approximately constant outside of the interval $[a, b]$, and the integral over $[a, b]$ itself. Then we can bound the approximations of $g(x)$ by their maximum values, pass the constants outside the integral, and evaluate integrals over a Gaussian distribution. Let us define the following:

$$\frac{1}{\sqrt{2\pi\sigma}} \exp\left(\frac{-1}{2\sigma}(z - \mu)^2\right) = C(z, \mu, \sigma) \quad (87)$$

$$\implies \int_a^b C(z, \mu, \sigma) = \frac{1}{2} \left(\operatorname{erf}\left(\frac{b - \mu}{\sqrt{2\sigma}}\right) - \operatorname{erf}\left(\frac{a - \mu}{\sqrt{2\sigma}}\right) \right) \quad (88)$$

Now we can compute an error bound over the mean of the output distribution by applying the triangle inequality, assumptions about the tail behavior of \tanh , our approximation over the interval $[a, b]$.

$$\begin{aligned} \left| \int_{-\infty}^{\infty} (g(z) - \tilde{g}(z))C(z, \mu, \sigma)dz \right| &\leq \left| \int_{-\infty}^a (g(z) - \tilde{g}(z))C(z, \mu, \sigma)dz \right| \\ &+ \left| \int_a^b (g(z) - \tilde{g}(z))C(z, \mu, \sigma)dz \right| \\ &+ \left| \int_b^{\infty} (g(z) - \tilde{g}(z))C(z, \mu, \sigma)dz \right| \end{aligned} \quad (89)$$

$$\begin{aligned} &\leq \left| \int_{-\infty}^a |\tanh(a) - (-1)|C(z, \mu, \sigma)dz \right| \\ &+ \left| \int_a^b \|g(z) - \tilde{g}(z)\|_{\infty}C(z, \mu, \sigma)dz \right| \\ &+ \left| \int_b^{\infty} |\tanh(b) - 1|C(z, \mu, \sigma)dz \right| \end{aligned} \quad (90)$$

$$\begin{aligned} &\leq c_1 \left(\operatorname{erf}\left(\frac{b-\mu}{\sqrt{2}\sigma}\right) - \operatorname{erf}\left(\frac{a-\mu}{\sqrt{2}\sigma}\right) \right) \\ &+ c_2 \left(\operatorname{erf}\left(\frac{a-\mu}{\sqrt{2}\sigma}\right) + 1 \right) \\ &+ c_3 \left(1 - \operatorname{erf}\left(\frac{b-\mu}{\sqrt{2}\sigma}\right) \right) \end{aligned} \quad (91)$$

$$= \epsilon_{\mu} \quad (92)$$

where $c_1 = \frac{1}{32}\tau^4 \|g^{(4)}(z)\|_{\infty}$, $c_2 = \frac{|1+\tanh(a)|}{2}$, $c_3 = \frac{|\tanh(b)-1|}{2}$. We can generalize this bound to any function in the expectation, we simply have to compute the appropriate polynomial coefficients and have an assumption about the tail behavior of the function. For example, let us additionally compute a bound for the variance. Let μ_{true} denote the true value of the mean, μ_{spline} be the approximated value of the mean. Additionally, let $\tilde{g}(z)$ be our polynomial approximation of $\tanh(z)^2$. Then we go to the expression for variance Equation (78):

$$\begin{aligned} \left| (\mathbf{E}((\tanh z)^2) - \mu_{true}^2) - (\mathbf{E}(\tilde{g}(z)) - \mu_{spline}^2) \right| &\leq \left| \mathbf{E}((\tanh z)^2 - \tilde{g}(z)) \right| + \left| \mu_{spline}^2 - \mu_{true}^2 \right| \\ &= \left| \mathbf{E}((\tanh z)^2 - \tilde{g}(z)) \right| + \\ &\quad \left| (\mu_{spline} - \mu_{true})(\mu_{spline} + \mu_{true}) \right| \end{aligned} \quad (93)$$

In this case, we apply Equation (91) with the coefficients of the integrand function $g(z) = \tanh(z)^2$, thus we can come up with a bound for the following integral in Equation (95):

$$\left| \int_{-\infty}^{\infty} (\tanh(z)^2 - \tilde{g}(z))C(z, \mu, \sigma)dz \right| \leq \epsilon_1 \quad (94)$$

Additionally, we know that $|\mu_{spline} - \mu_{true}| < \epsilon_{\mu}(a, b, \mu, \sigma, \tau)$ and that since we are dealing with the \tanh activation function, the activation mean is upper bounded by 1. Thus:

$$\left| \mathbf{E}((\tanh z)^2 - \tilde{g}(z)) \right| + \left| (\mu_{spline} - \mu_{true})(\mu_{spline} + \mu_{true}) \right| \leq \epsilon_1 + 2\epsilon_{\mu} = \epsilon_{\sigma} \quad (95)$$

Utilizing this method allows us to design the number of uniformly spaced mesh points and the size of the interval according to a desired accuracy. For reference, we utilize the interval $[-10, 10]$ for the mean of the \tanh activation, and use 101 mesh points, resulting in an error bound of $4.21321e-5$ for the mean of an input distribution with mean 3 and variance 0.2.

6.2 Probabilistic Echo State Networks

The proposed algorithm, Probabilistic Echo State Networks (PESN) derives its internal equations from the deterministic echo state network [13]. Let $z_k \in \mathbb{R}^{N_x+N_u}$ be input to the network, $y_k \in \mathbb{R}^{N_x}$ be the output of the network, $h_k \in \mathbb{R}^{N_h}$ is the hidden state at time k . The deterministic echo state network is characterized by 5 hyperparameters: reservoir size N_h , leak rate L , noise magnitude M_e , sparsity fraction s , and spectral radius r .

$$h_k = (1 - L)h_{k-1} + L \tanh(W_{\text{in}}z_k + W_{\text{fb}}y_{k-1} + Wh_{k-1}) + M_e dw \quad (96)$$

$$y_k = W_{\text{out}} [1 \quad z_k^T \quad h_k^T]^T \quad (97)$$

Here dw is Gaussian noise with variance 1. The sparsity fraction refers to the fraction on nonzero elements in the matrix W , while the spectral radius parameter is the spectral radius of W . For the echo state network, we randomly generate the internal weight matrices W_{in} , W_{fb} , and W , and we only train the readout weight matrix W_{out} . In our case, training is accomplished using batch least squares. At test time, we recursively update the readout matrix using recursive least squares regression. [18]

We now present expressions for probabilistic echo state networks. Here we assume that in that the input to the networks are Gaussian, we use moment matching to propagate the Gaussian uncertainty through the nonlinearity in the network, and we are able to retrieve a Gaussian output. Our notation is as follows: a Gaussian random vector \mathbf{z} has a mean $\mu_{\mathbf{z}}$ and covariance matrix $\Sigma_{\mathbf{z}}$. We assume that all Gaussian vectors in our echo state network are additionally jointly Gaussian, so that linear combinations of these Gaussian vectors produce another Gaussian vector with appropriate mean vector and covariance vector. That is if \mathbf{a} and \mathbf{b} are Gaussian random vectors that are also jointly Gaussian, then:

$$\mathbf{c} = W_1\mathbf{a} + W_2\mathbf{b} \quad (98)$$

$$\mu_{\mathbf{c}} = W_1\mu_{\mathbf{a}} + W_2\mu_{\mathbf{b}} \quad (99)$$

$$\Sigma_{\mathbf{c}} = W_1\Sigma_{\mathbf{a}}W_1^T + W_2\Sigma_{\mathbf{b}}W_2^T + 2W_1\Sigma_{\mathbf{ab}}W_2^T \quad (100)$$

Analogously to Equation (96) if the input is given by $\mathbf{z}(k)$, the previous target by $\mathbf{y}(k-1)$ and the hidden state by $\mathbf{h}(k-1)$, the argument to the activation function is given by

$$\mathbf{a} = W_{\text{in}}\mathbf{z}(k) + W_{\text{fb}}\mathbf{y}(k-1) + W\mathbf{h}(k-1) \quad (101)$$

$$\mu_{\mathbf{a}} = W_{\text{in}}\mu_{\mathbf{z}(k)} + W_{\text{fb}}\mu_{\mathbf{y}(k-1)} + W\mu_{\mathbf{h}(k-1)} \quad (102)$$

$$\begin{aligned} \Sigma_{\mathbf{a}} = & W_{\text{in}}\Sigma_{\mathbf{z}(k)}W_{\text{in}}^T + W_{\text{fb}}\Sigma_{\mathbf{y}(k-1)}W_{\text{fb}}^T + W\Sigma_{\mathbf{h}(k-1)}W^T \\ & + 2W_{\text{in}}\Sigma_{\mathbf{z}(k)\mathbf{y}(k-1)}W_{\text{fb}}^T + 2W_{\text{fb}}\Sigma_{\mathbf{y}(k-1)\mathbf{h}(k-1)}W^T + 2W\Sigma_{\mathbf{h}(k-1)\mathbf{z}(k)}W_{\text{in}}^T \end{aligned} \quad (103)$$

Using our element-wise approximation, we drop the off-diagonal terms in \mathbf{a} and compute the approximate mean $\mu_{\tanh(\mathbf{a})}$ and variance $\Sigma_{\tanh(\mathbf{a})}$ using Equations (77) and (78).

$$\mathbf{h}(k) = (1 - L)\mathbf{h}(k-1) + L \tanh(\mathbf{a}) + M_e dw \quad (104)$$

$$\mu_{\mathbf{h}(k)} = (1 - L)\mu_{\mathbf{h}(k-1)} + L\mu_{\tanh(\mathbf{a})} \quad (105)$$

$$\Sigma_{\mathbf{h}(k)} = (1 - L)^2\Sigma_{\mathbf{h}(k-1)} + L^2\Sigma_{\tanh(\mathbf{a})} + 2(1 - L)L\Sigma_{\tanh(\mathbf{a})\mathbf{h}(k-1)} + M_e\mathbf{I} \quad (106)$$

The leaky hidden state is given by Equation (104), then we can construct the readout input $\mathbf{b} = [1, \mathbf{z}^T, \mathbf{h}^T]^T$

$$\mathbf{y}(k) = W_{\text{out}}\mathbf{b} \quad (107)$$

$$\mu_{\mathbf{y}(k)} = W_{\text{out}}\mu_{\mathbf{b}} \quad (108)$$

$$\Sigma_{\mathbf{y}(k)} = W_{\text{out}}\Sigma_{\mathbf{b}}W_{\text{out}}^T \quad (109)$$

Here (N_h, L, M_e, s, r) are the five hyperparameters for the echo state network, z and y are input and output data, generated or collected from experiments, n_{train} and n_{test} are the lengths of the train and test data, λ is a forgetting factor, P is δI where I is the identity matrix, W_{in} , W_{out} , W_{fb} , and W are the weights of the network, h is the hidden state.

6.3 Experimental Evaluation

6.3.1 Activation Function Moment Comparison

First we compare the absolute error between the mean and variance estimated from Monte Carlo against the mean and variance from spline method and analytic method. We evaluate our moment

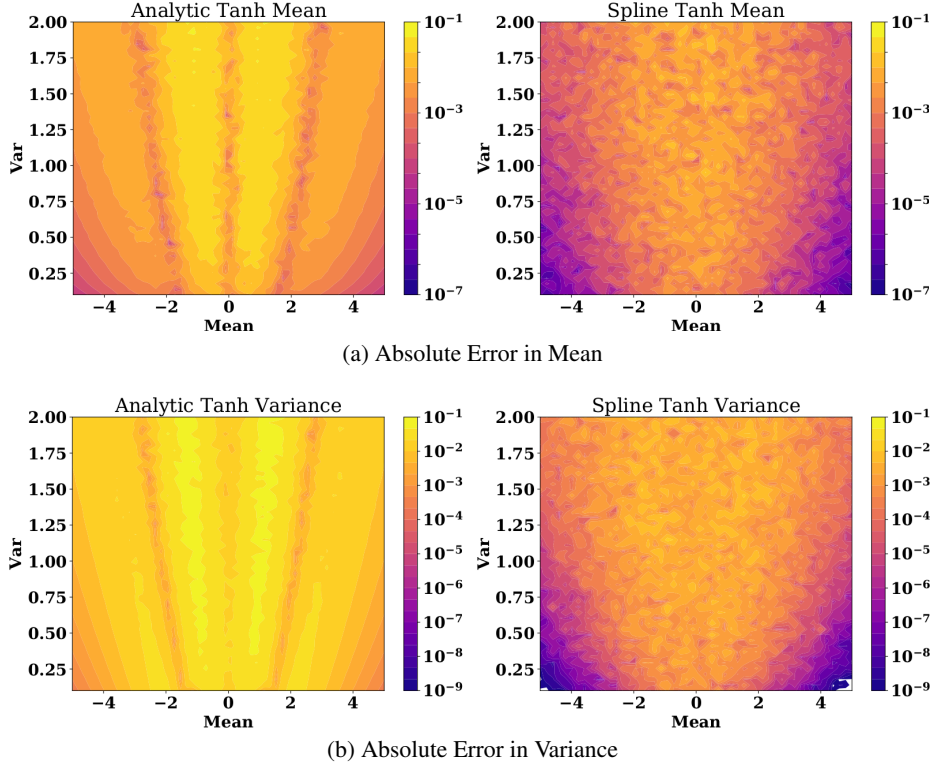


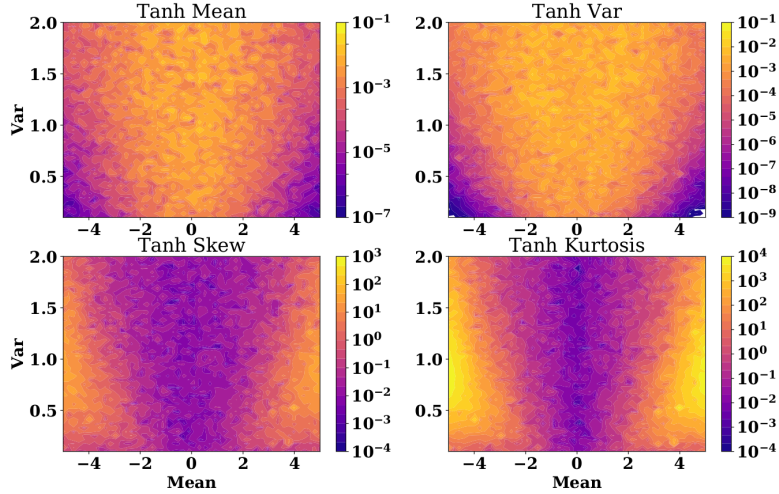
Figure 4: Absolute Error in Moment Comparison between the analytic (left) and spline (right) methods of propagating uncertainty through the tanh. Note that the color bar is in log scale, where darker color implies lower error.

propagation on a grid of input means and variances to assess accuracy on a range. At each gridpoint, we have an input Gaussian distribution determined by a mean and variance. We sample this input distribution and compute an estimated mean and variance through Monte Carlo, then compare against our two methods. Figure 4 shows that the spline method results in a more accurate approximation, and as the input saturates (mean approaches 5 and -5), the error quickly drops logarithmically. In general we see the analytic approximation over estimates the variance of the tanh output.

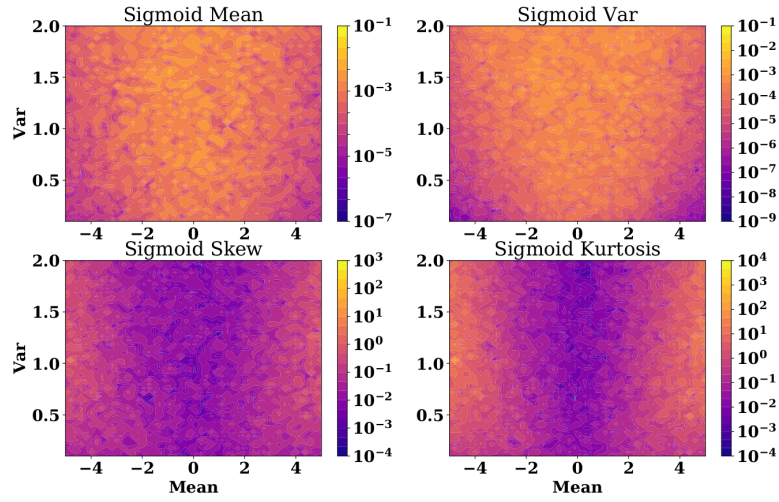
Additionally, we can compute the skew and kurtosis any continuous activation function. The expressions for these moments are given in Equations (77) - (80). We present the absolute error in moments for mean, variance, skew, and kurtosis for 3 activation functions utilizing the spline method: tanh, *sigmoid*, and *swish* (where $\beta = 1$ for the swish activation function) in Figure 5.

6.3.2 Multiple Layer Uncertainty Propagation

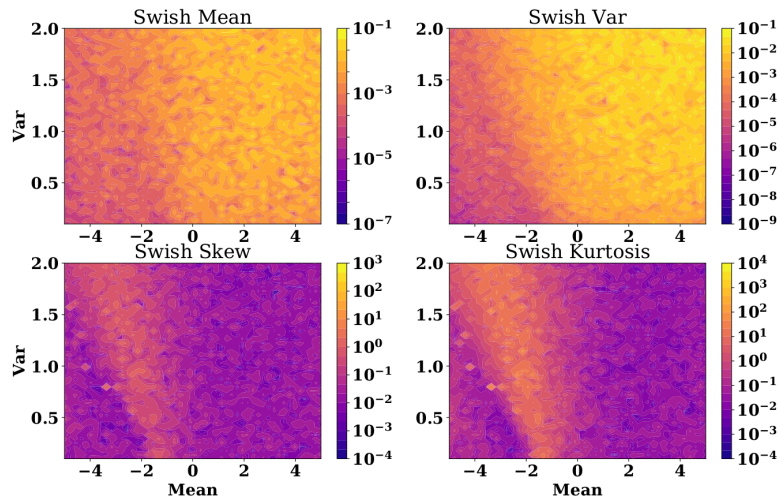
In this section, we have constructed two feedforward neural networks with the tanh activation function to demonstrate the performance of the moment approximations. In this case, we randomly initialized all weight matrices. In both cases, the network input is 1024 units and the network output is a single unit. Network 1 has a width of 5 units for 5 hidden layers and network 2 has a width of 50 units and 10 hidden layers. The uncertain input is Gaussian distributed with mean -0.5, and variance 0.01. We see in Table 4a that for network 1, the output is close to a delta function, as a result of the saturation of neurons. The analytical method over estimates the variance in this case, while the spline method is able to recover the moments well. For network 2, shown in Table 4b, the distribution goes from a delta function to Gaussian, and both the analytical method and the spline method can recover the output distribution. We see in the table, the absolute error of approximation is smaller for the spline case. Our error criteria are defined for a given approximation \hat{X} , layer i , and number of hidden units N_{hi} . $\mu_{MC,i,j}$ is the Monte Carlo approximation mean at layer i , hidden unit j . The Monte Carlo



(a) Tanh



(b) Sigmoid



(c) Swish

Figure 5: Absolute Error in Mean, Variance, Skew and Kurtosis. Again note that the color bar is in log scale, where darker color implies lower error. We have large errors in skew and kurtosis wherever the variance is less than $10e - 6$, since these moments are standardized using the variance.

approximation was computed with 50000 samples.

$$\epsilon_{\mu_X,i} = \frac{1}{N_{hi}} \sum_{j=1}^{N_{hi}} |\mu_{MC,i,j} - \mu_{X,i,j}| \quad (110)$$

$$\epsilon_{\sigma_X,i} = \frac{1}{N_{hi}} \sum_{j=1}^{N_{hi}} |\sigma_{MC,i,j} - \sigma_{X,i,j}| \quad (111)$$

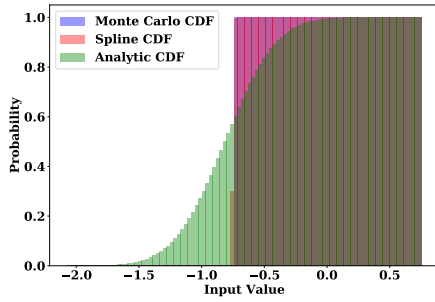
Table 4: Absolute Error Statistics for FFNN. Subscript ‘‘S’’ represents the spline method, while ‘‘A’’ represents the analytical method. The input is 1024 units, and the output is 1 unit. The uncertain input is Gaussian distributed with mean -0.5, and variance 0.01.

(a) Shallow Network with 5 Hidden Units and 5 Layers

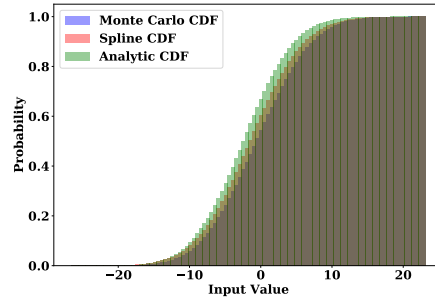
Error Statistics	Layers					
	1	2	3	4	5	Out
μ_S	2.24e-05	4.09e-05	3.08e-05	5.02e-05	6.02e-05	2.04e-05
μ_A	8.91e-04	8.82e-04	9.77e-03	1.12e-02	1.43e-02	6.26e-02
σ_S	3.31e-05	5.98e-05	3.48e-05	2.66e-05	2.04e-05	7.43e-05
σ_A	1.79e-03	2.10e-02	1.20e-02	1.99e-02	2.54e-02	1.05e-01

(b) Deep Network with 50 Hidden Units and 10 Layers

Error Statistics	Layers					Out
	1	3	5	7	9	
μ_S	7.97e-04	1.01e-02	5.19e-02	7.99e-02	8.27e-02	9.81e-02
μ_A	5.98e-03	1.58e-02	5.06e-02	7.48e-02	8.16e-02	1.05e-01
σ_S	1.03e-03	6.60e-02	7.50e-02	7.11e-02	3.90e-02	5.30e-01
σ_A	8.44e-03	6.64e-02	7.13e-02	9.57e-02	7.13e-02	2.95e+00



(a) Shallow Network CDF



(b) Deep and Wide Network CDF

Figure 6: CDF comparison for two different networks. In the shallow network, the output cdf is close to a delta function. In the deep and wide network, the output cdf is close to a Gaussian distribution.

6.3.3 Model learning

In the field of robotics and autonomy, recently there is an increasing interest in using machine learning to get the accurate model approximation. Model accuracy is important for many applications including planning and control. However, analytical models cannot catch the complexity of a system very well, so we approximate the system model by learning from data. In this section, we learn unknown system dynamics from data using probabilistic echo state networks(ESN) and evaluate the learned model. We suppose our systems’ dynamics are unknown and represent the dynamics as the following differential equation

$$dx = f(x, u)dt + C(x, u)dw, \quad dw \sim \mathcal{N}(0, \Sigma_\omega) \quad (112)$$

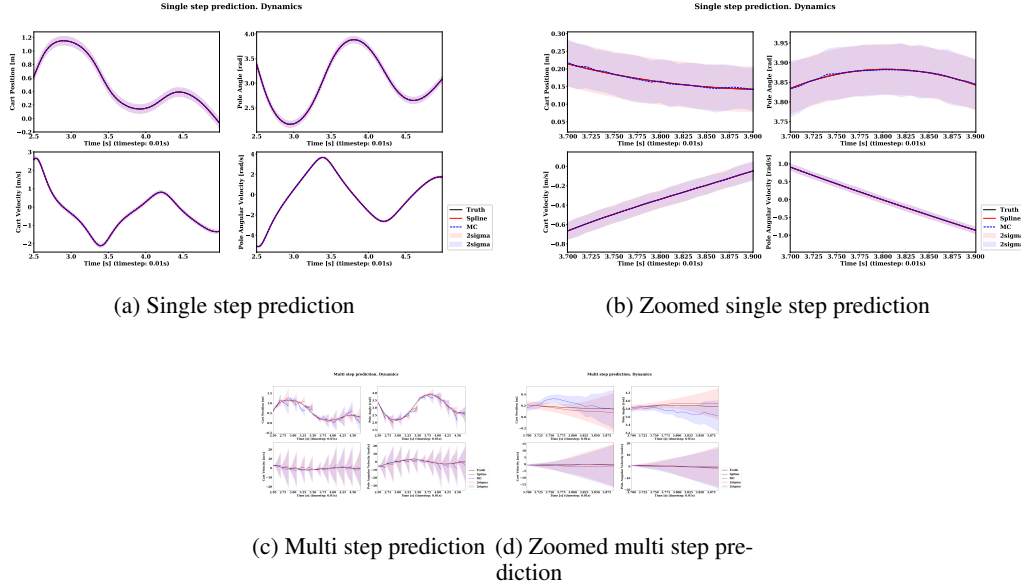


Figure 7: Cart pole state transition prediction. The red line and shadow represent the predicted mean and 2σ (standard deviation) from probabilistic ESN using spline-approximated \tanh . The blue line and shadow are from MC sampling of deterministic ESN under uncertain inputs. Multi step prediction plots 20 time steps starting from the ground truth(black).

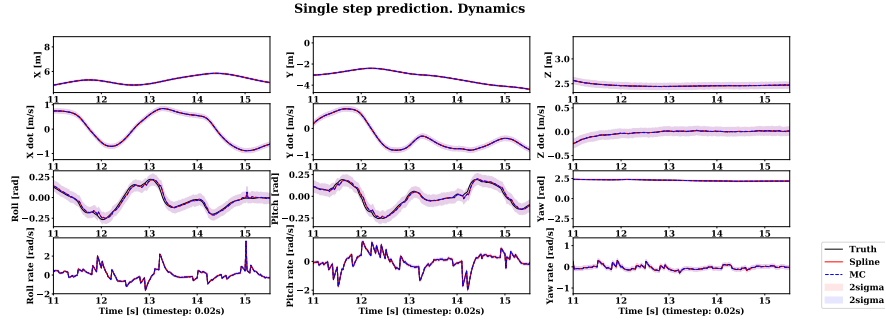
,where $\mathbf{x} \in \mathbb{R}^{N_x}$ is the state and $\mathbf{u} \in \mathbb{R}^{N_u}$ is the control. Given the state-control pair and the state transition $d\mathbf{x}$, we are able to infer the dynamics as well as the state transition. With the goal of inferring $d\mathbf{x}$ given (\mathbf{x}, \mathbf{u}) , we compare our probabilistic ESN using spline approximation of \tanh to Monte Carlo(MC) sampling of the deterministic ESN using \tanh under uncertain inputs. To make the inputs uncertain for the deterministic ESN, we added Gaussian noise to the state \mathbf{x} when we do the MC sampling. For fair comparison, the two networks shared same weights W_{in}, W_{out}, W_{fb} , and W . Data for the Cart Pole system was generated by equations of motion derived using first principles and the ARDrone data was collected using a Gazebo simulator [20]. As the kinematics of each system is straightforward and easy to derive, we directly use the kinematics equations to predict next position states and we only learn the dynamics of the systems with ESNs.

Cart Pole: We consider the Cart Pole having a state vector $\mathbf{x} = [x, \theta, \dot{x}, \omega]^T$, where x is cart position, θ is pole angle, \dot{x} is cart velocity and ω is pole angular velocity. The control input to the system \mathbf{u} is the force applied to the cart. Through several times of simulation with different controls, we collected various data. We use $[\mathbf{x}^T, \mathbf{u}^T]^T$ as an input to the network. To learn the dynamics of the system, we set the target output as the two velocity terms $[\dot{x}, \omega]^T$.

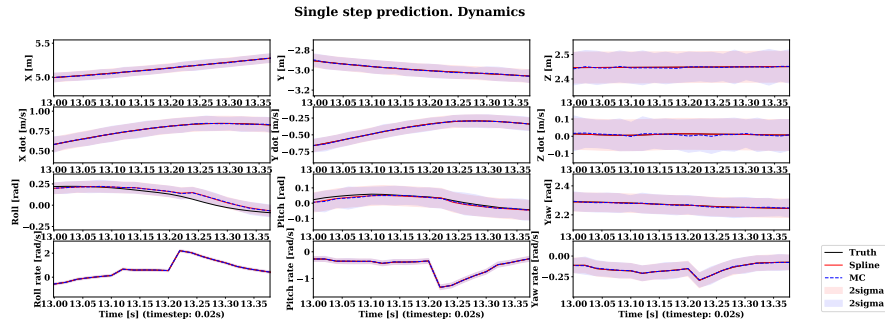
ARDrone: In the simulated ARDrone, we use 12 state of the system. $\mathbf{x} = [x, y, z, \dot{x}, \dot{y}, \dot{z}, \phi, \theta, \psi, \dot{\phi}, \dot{\theta}, \dot{\psi}]^T$, where (x, y, z) are positions, (ϕ, θ, ψ) are angles, $(\dot{x}, \dot{y}, \dot{z})$ are linear velocities and $(\dot{\phi}, \dot{\theta}, \dot{\psi})$ are roll rate, pitch rate and yaw rate each. The control input to the ARDrone system is $\mathbf{u} = [v_{x,cmd}, v_{y,cmd}, v_{z,cmd}, v_{\psi,cmd}]^T$. Here $(v_{x,cmd}, v_{y,cmd}, v_{z,cmd})$ are linear x, y, z velocity commands and $v_{\psi,cmd}$ is the angular z velocity command. Running the simulated ARDrone with various control commands, we collected 80,000+ data. Using $[\mathbf{x}^T, \mathbf{u}^T]^T$ as an input to the network, we set the output target as velocity terms $[\dot{x}, \dot{y}, \dot{z}, \dot{\phi}, \dot{\theta}, \dot{\psi}]^T$ to learn the dynamics of the drone.

6.3.4 Discussion

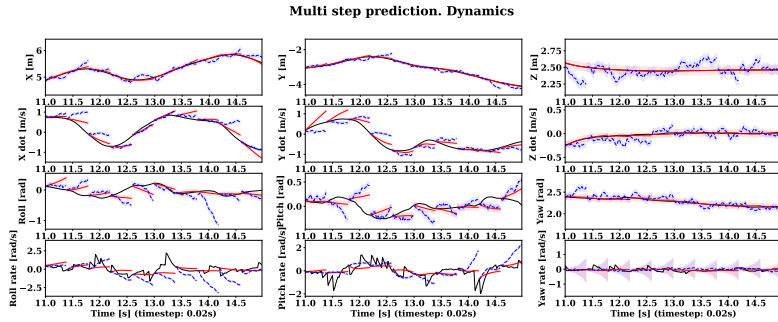
Figure 7 and 8 shows the results of single step and multi step predictions of state transitions from the learned Cart Pole and ARDrone models using probabilistic and deterministic echo state networks. As the probabilistic ESN and the deterministic ESN use the same weights of the trained model, the probabilistic ESN can propagate uncertainty successfully as Monte Carlo method does. In the single step prediction of both systems, the probabilistic ESN almost perfectly captures the output mean and



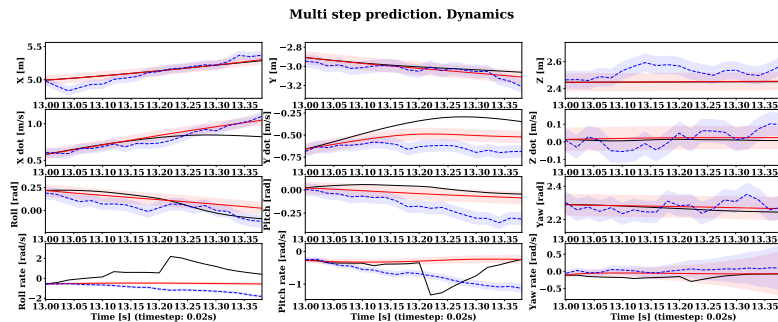
(a) Single step prediction



(b) Zoomed single step prediction



(c) Multi step prediction



(d) Zoomed multi step prediction

Figure 8: ARDrone state transition prediction. The red line and shadow represent the predicted mean and 2σ (standard deviation) from probabilistic ESN using spline-approximated \tanh . The blue line and shadow are from MC sampling of deterministic ESN under uncertain inputs. Multi step prediction plots 20 time steps starting from the ground truth(black).

variance of the MC-sampled deterministic ESN with uncertain inputs. However, in the multi step prediction, the predicted mean of probabilistic ESN diverges from the MC-sampled ESN after 4-5 time steps, but the variance of the distribution grows similarly.